16. Rios MA, Fernández A, Tormo BR, et al. Heterogenous expression of the EGF receptor in human breast carcinoma. *Anticancer Res* 1992;12:205–208.
17. Neal DE, March C, Benett MK, et al. Epidermal growth factor receptors in human bladder cancer. Comparison of invasive and superficial tumors. *Lancet* 1985;i:346–348.
18. Magnusson I, Rosen AV, Nilsson R, Macias A, Pérez R, Skoog L. Receptors for epidermal growth factor and sex steroid hormones in human colorectal carcinomas. *Anticancer Res* 1989;9:299–302.
19. Veale D, Ashcroft T, March C, Gibson GJ, Harris AL. Epidermal growth factor receptors in non-small cell lung cancer. *Br J Cancer* 1987;55:513–516.
20. Fernández A, Pérez R, Macias A, et al. Generación y caracterización primaria de anticuerpos monoclonales contra el receptor del factor de crecimiento epidérmico. *Interferón Biotecnol* 1989;6:289–299.
21. Fernández A, Spitzer E, Pérez R, et al. A new monoclonal antibody for detection of EGF-receptors in Western blots and paraffin-embedded tissue sections. *J Cell Biochem* 1992;49:157–165.
22. Iznaga-Escobar N, Morales A, Núñez G. Micromethod for quantification of SH groups generated after reduction of monoclonal antibodies. *J Nucl Med Biol* 1996;23:641–644.
23. Pearson TC, Guthrie DL, Simpson J, et al. Interpretation of measured red cell mass and plasma volume in adults. *Br J Haematol* 1995;89:748–756.
24. Dubois D, Dubois EF. A formula to estimate the approximate surface area if height and weight be known. *Arch Intern Med* 1916;17:863–871.
25. Jennrich RI, Sampson PF. Application of stepwise regression to nonlinear least squares estimation. *Techometrics* 1968;10:63–72.
26. Akaike A. Posterior probabilities for choosing regression model. *Ann Inst Math Stat* 1978;30:A9–A14.
27. Iznaga-Escobar N, Torres LA, Morales A, et al. Technetium-99m-labeled anti-EGF-receptor antibody in patients with tumor of epithelial origin. II. Pharmacokinetics and clearances. *J Nucl Med* 1998;39:in press.
28. Gibaldi M, Perrier D. Pharmacokinetics. In: Gibaldi M, Perrier D, eds. *Pharmacokinetics*, 2nd Ed. New York: Marcel Dekker Inc.; 1982:319–355.
29. Stabin MG. Patient dose from diagnostic and therapeutic radiopharmaceuticals. In: Raabe OG, ed. *Internal radiation dosimetry: Health Physics Society 1994 Summer School*. Madison, WI: Medical Physics Publishing; 1995:375–392.
30. Snyder WS, Ford MR, Warmer GG, Watson SB. *"S" absorbed dose per unit cumulated activity for selected radionuclides and organs*, MIRD Pamphlet No. 11. New York: Society of Nuclear Medicine; 1975.
31. Snyder WS, Ford MR, Warmer GG, Fisher HL. Estimates of absorbed fractions for monoenergetic photon sources uniformly distributed in various organs of a heterogeneous phantom. In: *Medical internal radiation dose (MIRD)*, Vol. 5. New York: Society of Nuclear Medicine; 1978:50–67.
32. International Commission on Radiological Protection (ICRP). *Limits for intakes of radionuclides by workers*, ICRP Publ. No. 30. New York: Pergamon Press; 1979:1–13.
33. International Commission on Radiological Protection (ICRP). *Recommendations of the International Commission on Radiological Protection*, ICRP Publ. No. 60. New York: Pergamon Press; 1991;21:1–3.
34. Baselga J, Mendelsohn J. The epidermal growth factor receptor as a target for therapy in breast carcinoma. *Breast Cancer Res Treat* 1994;29:127–138.
35. Khetarpal VK, Storbeck LS. Biological disposition of intravenously administered ^{131}I-labeled anti-EGF-receptor antibody (RG 83852) in rat. *Cancer Chemother Pharmacol* 1995;35:313–317.
36. Murthy U, Basu A, Rodeck U, Herlyn M, Ross AH, Das M. Binding of antagonistic monoclonal antibody to an intact and fragmented EGF-receptor polypeptide. *Arch Biochem Biophys* 1987;72:77–89.
37. Takahashi H, Nakazawa S, Herlyn D. Experimental radioimmunotherapy of a xenografted human glioma using ^{131}I-labeled monoclonal antibody to epidermal growth factor receptor. *Neurol Med Chir Tokyo* 1993;33:610–615.
38. Dadparvar S, Krishna L, Miyamoto C, et al. Indium-111-labeled anti-EGFr-425 scintigraphy in the detection of malignant gliomas. *Cancer* 1994;73(suppl):884–889.
39. Steiner K, Haunschild J, Faro HP, Senekowitsh R. Distribution of humanized MAb 425 (EMD 62 000) in rats and specific localization in tumor-bearing nude mice. *Cell Mol Biol* 1995;41:179–184.
40. Hammond ND, Moldofsky PJ, Bearsley MR, et al. External imaging techniques for quantitation of distribution of ^{131}I-labeled F(ab')$_2$ fragments of monoclonal antibody in humans. *Med Phys* 1984;11:778–783.
41. Eary JF, Appelbaum FL, Durack L, et al. Preliminary validation of the opposing view method for quantitative gamma camera imaging. *Med Phys* 1989;16:382–387.
42. Macias A, Pérez R, Lage A. Estudios sobre el factor de crecimiento epidérmico. II. Desarrollo de un radio-receptor análisis para la determinación de cantidades picomolares. *Interferón Biotecnol* 1985;2:115–127.
43. Kirkwood JM, Neumann RD, Zoghbi SS, et al. Scintigraphic detection of metastatic melanoma using indium-111/DTPA conjugated anti-gp240 antibody (ZME-018). *J Clin Oncol* 1987;5:1247–1255.
44. Wessels B, Rogus RD. Radionuclide selection and model absorbed dose calculations for radiolabeled tumor associated antibodies. *Med Phys* 1984;11:638–675.
45. Fisher DR, Badger CC, Breitz HB, et al. Internal radiation dosimetry for clinical testing of radiolabeled monoclonal antibodies. *Antibody Immunoconj Radiopharm* 1991;4:655–664.
46. Epenetos AA, Snook D, Durbin H, Johnson PM, Taylor-Papadimitriou J. Limitations of radiolabeled monoclonal antibodies for localization of human neoplasms. *Cancer Res* 1986;46:3183–3191.
47. Dykes PW, Bradwell AR, Chapman CE, Vaughan ATM. Radioimmunotherapy of cancer: clinical studies and limiting factors. *Cancer Treat Rev* 1987;14:87–106.
48. Leichner PK, Klein JL, Garrison JB, et al. Dosimetry of ^{131}I-labeled anti-ferritin in hepatoma: a model for radioimmunoglobulin dosimetry. *Int J Radiat Oncol Biol Phys* 1981;7:323–333.
49. Beaumier PC, Venkatesan P, Vanderheyden JL, et al. Re-186 radioimmunotherapy of small cell lung carcinoma xenografts in nude mice. *Cancer Res* 1991;51:676–681.
50. Griffiths GL, Goldenberg DM, Knapp FF Jr, et al. Direct radiolabeling of monoclonal antibodies with generator-produced rhenium-188 for radioimmunotherapy: labeling and animal biodistribution studies. *Cancer Res* 1991;51:4594–4602.

Diagnosis of Recurrent Glioma with SPECT and Iodine-123-α-Methyl Tyrosine

Torsten Kuwert, Burkhard Woesler, Carlo Morgenroth, Hartmut Lerch, Michael Schäfers, Stefan Palkovic, Peter Matheja, Wolfgang Brandau, Hansdetlef Wassmann and Otmar Schober

Departments of Nuclear Medicine and Neurosurgery, Westfälische Wilhelms-Universität, Münster, Germany

Iodine-123-α-methyl tyrosine (IMT) allows the investigation of amino acid transport rate in brain neoplasms. It was the aim of this study to evaluate the potential of IMT-SPECT to diagnose the recurrence of gliomas after primary therapy. **Methods:** Using a triple-headed SPECT camera, the cerebral uptake of IMT was determined in 27 patients 22 mo, on average, after surgical removal of a primary brain tumor. Eighteen patients had suffered from high-grade gliomas, and nine had suffered from low-grade tumors. Four patients were examined before and after surgical revision of a presumed tumor recurrence. A total of 31 studies were evaluated. The final diagnosis was based on prospective clinicopathological follow-up. Recurrence was diagnosed in 23 cases, with marked clinical deterioration occurring 3.1 mo, on average, after SPECT, and was confirmed by histopathology in 14 instances. Eight cases were free of recurrence, as evidenced by inconspicuous clinical follow-up, ranging from 6 mo to 17 mo after SPECT in seven cases, and by clinical course and histopathology in the remaining subject. **Results:** Patients with recurrence had significantly higher ratios of IMT uptake in the tumor area to that in a background region than did patients without recurrence (2.27 ± 0.59 compared to 1.47 ± 0.29; $p < 0.002$). The best cutoff level of the IMT uptake ratio in the differentiation between recurrence and benign posttherapeutic lesion was 1.8. Using this study-specific discrimination threshold, the sensitivity and specificity of IMT-SPECT for detecting glioma recurrence were 18 of 23 (78%) and 8 of 8 (100%), respectively. The area under the binormal receiver operating characteristic curve, fitted to the data, was 0.90 ± 0.06. **Conclusion:** Iodine-123-α-methyl tyrosine-SPECT is a promising new tool in the follow-up of patients with gliomas after primary therapy.

Key Words: SPECT; iodine-123-α-methyl tyrosine; amino acids; brain neoplasms; gliomas

J Nucl Med 1998; 39:23–27

Received Oct. 28, 1996; revision accepted Mar. 14, 1997.

For correspondence or reprints contact: Torsten Kuwert, MD, Department of Nuclear Medicine, Westfälische Wilhelms-Universität Münster, Albert-Schweitzer-Strasse 33, 48129 Münster, Germany.

TABLE 1
Patient Clinical Data

Patient no.	Age (yr)	Sex	Initial histology	Radiotherapy (Gy)	Time between initial surgery and SPECT (mo)	Diagnosis (mo)	Method verification (mo)*	MRI/CT	IMT-SPECT uptake†
1	70	M	Oligo II	None	4	N	Follow-up (10)	C	1.49
2	34	F	Astrocytoma II	None	23	N	Follow-up (6)	NC	0.88
3A	47	F	Radionecrosis	60 + IORT	4	N	Follow-up (6)	C	1.70
3B	47	F	Ependymoma III	60 + IORT	20	N	Surgery (1)	C	1.75
4	51	M	Astrooligo III	60	12	N	Follow-up (13)	NC	1.65
5	52	M	Astrocytoma III	60 + IORT	9	N	Follow-up (17)	C	1.23
6	53	M	Astrocytoma IV	60 + IORT	4	N	Follow-up (7)	C	1.55
7	51	F	Astrocytoma IV	40 + IORT	8	N	Follow-up (13)	C	1.49
8	53	F	Oligo II	56	216	R	Surgery (10)	NC	2.63
9	26	M	Oligo II	None	12	R	Surgery (2)	NC	1.44
10	51	M	Oligo II	60	78	R	Follow-up (3)	C	3.24
11A	35	M	Oligo II	None	47	R	Surgery (1)	C	2.57
11B	36	M	Oligoastro II	None	12	R	Surgery (1)	C	2.54
12	50	M	Oligoastro II	60	14	R	Follow-up (13)	C	2.86
13	48	F	Astrooligo II	None	8	R	Follow-up (3)	NC	2.60
14	72	F	Astrocytoma II	None	11	R	Surgery (1)	C	3.23
15	50	F	Oligo III	60	67	R	Follow-up (10)	C	2.45
16	58	M	Astrooligo III	30 + 60 + IORT	9	R	Surgery (1)	C	2.68
17	38	M	Astrocytoma III	50 + IORT	17	R	Surgery (1)	C	1.58
18	63	F	Astrocytoma III	60	24	R	Surgery (1)	C	2.15
19	34	M	Astrocytoma III	20 + Brachy	10	R	Surgery (1)	C	2.71
20	66	F	Astrocytoma III	60	6	R	Surgery (1)	C	1.83
21	58	M	Astrocytoma III	60	3	R	Follow-up (4)	C	1.65
22	62	M	Astrocytoma IV	60	7	R	Surgery (1)	C	1.99
23A	56	F	Astrocytoma IV	60	11	R	Surgery (1)	C	2.87
23B	56	F	Astrocytoma IV	60 + IORT	7	R	Follow-up (5)	C	1.58
24	48	F	Astrocytoma IV	60	12	R	Surgery (2)	C	2.24
25A	49	M	Astrocytoma IV	56	10	R	Surgery (1)	C	2.64
25B	49	M	Astrocytoma IV	60 + IORT	3	R	Follow-up (3)	C	1.88
26	51	M	Astrocytoma IV	60 + IORT	6	R	Follow-up (5)	C	0.98
27	58	M	Astrocytoma IV	60	5	R	Follow-up (1)	C	1.88

*Number in parentheses defines the time between IMT-SPECT and surgery or month of follow-up, respectively.

†IMT uptake in the tumor area divided by that in a background region.

M = male; F = female; Oligo = oligodendroglioma; Astrooligo = astrooligodendroglioma; Oligoastro = oligoastrocytoma; IORT = intraoperative radiotherapy (20 Gy); Brachy = brachytherapy; N = no recurrence; R = recurrence; C = contrast enhancement; NC = no contrast enhancement.

The primary therapy of gliomas consists of surgery and a combination of radiotherapy and chemotherapy (*1*). On follow-up, the differential diagnosis between recurrence or regrowth of residual tumor on one hand and benign post-therapeutic lesions on the other presents particular problems because x-irradiation CT and magnetic resonance imaging (MRI) frequently fail to differentiate between these two conditions (*2–4*). Therefore, the use of radionuclide imaging has been advocated for this purpose; in particular, PET with ^{18}F-fluorodeoxyglucose (FDG) has been shown to be useful in this regard (*5,6*).

However, PET is extremely expensive and is of only limited availability. Therefore, research has concentrated on developing conventional radiopharmaceuticals that are capable of imaging variables that are associated with tumor metabolism. Recently, the radioactively labeled amino acid ^{123}I-α-methyl tyrosine (IMT) has been introduced for the investigation of amino acid transport rate in gliomas with SPECT (*7–10*). The first clinical studies with this radiopharmaceutical have demonstrated that IMT-SPECT is suitable for grading gliomas in an analogous manner to FDG-PET and may help in the differential diagnosis between non-neoplastic lesions and high-grade gliomas (*11,12*).

This study evaluates the potential of IMT-SPECT to diagnose the recurrence of brain tumors after primary therapy.

MATERIALS AND METHODS

Patients

Twenty-seven patients were entered into the study after primary therapy for gliomas over a period of 28 mo. Informed consent was obtained from every subject. The study protocol had been approved by the Ethical Committee of the Westfälische Wilhelms-Universität (Münster, Germany).

Clinical and demographic data are detailed in Table 1. The group studied included 10 patients with an initial tumor grade of II, according to the revised classification scheme of the World Health Organization (WHO) (*13*), and 17 patients with an initial diagnosis of a glioma III or IV. Three patients with high-grade gliomas (Patients 3, 23 and 25) and one patient with a low-grade glioma (Patient 11) were examined before and after surgical revision of a presumed tumor recurrence. A total of 31 studies were evaluated.

The final diagnosis was based on prospective clinicopathological follow-up, evaluated by two board-certified neurological surgeons, independently of the IMT-SPECT data. Eight cases were free of recurrence, as evidenced by inconspicuous clinical follow-up, ranging from 6–17 mo after SPECT. In one of these (Patient 3A), surgical reintervention was performed in spite of her unremarkable clinical follow-up due to marked enlargement of the contrast-

enhancing zone on MR; histopathology was that of a radionecrosis. Recurrence was diagnosed in 23 cases, with marked clinical deterioration occurring 3.1 mo, on average, after SPECT, with a range of 1–13 mo. In 14 of these cases, open surgery (12 cases) or stereotactic biopsy (2 cases) confirming this diagnosis was performed 37 days, on average, after SPECT, encompassing a range of 1–302 days (Table 1).

In all patients, contrast-enhanced MRI or CT (Patients 3A, 8, 15, 24, 25B and 26) was performed 14.5 days, on average, within IMT-SPECT before any therapeutic reintervention (range, 2–40 days). Contrast enhancement was noted in 20 of 23 cases with a clinical diagnosis of recurrence and in 6 of 8 instances with unremarkable clinical course (Table 1).

SPECT Data Acquisition

Details of the performance of IMT-SPECT in our laboratory have been described and discussed previously (*11,12*) so that only a brief description need be given here.

The patients fasted at least 4 hr before IMT injection. SPECT was performed using the triple-headed camera MULTISPECT 3 (Siemens Gammasonics), equipped with medium-energy collimators (*14*). Imaging was started 10 min after intravenous injection of 110 MBq–130 MBq of IMT, synthesized and purified as reported previously (*15,16*); 96 views (3 × 32; 3.75°/step), each registered over 60 sec, were recorded into a 128 × 128 matrix format that corresponded to a pixel dimension of 3.56 × 3.56 mm on a 360° rotation. Transaxial tomograms were reconstructed without prefiltering using filtered backprojection. Attenuation correction was first-order, applying the method of Chang (*17*). In-plane resolution of the reconstructed images was 14 mm FWHM, and slice thickness was approximately 7 mm.

Data Analysis

Without knowledge of the clinical and histopathological data, regions of interest (ROIs) were manually defined on the two transaxial tomograms with the highest uptake of the lesion under study. As described and discussed in more detail previously (*11,12*), the ROIs placed on the lesions encompassed all pixels within that lesion with uptake values greater than 90% of the maximum uptake in that slice. This approach to measuring regional radiotracer uptake was introduced by Rottenberg et al. (*18*) and is also used by other groups to quantify the uptake of radiolabeled amino acids by brain tumors (*19*). In three patients (Patients 2, 5 and 26), there were no pixels with an IMT uptake greater than 90% of the slice's maximum within the lesional area; in these subjects, the ROI was placed with close reference to CT or MRI. The further analysis resided on the average counting rate in each ROI. Mean ROI size was 6.0 cm^2, with a median of 4.6 cm^2 and a range from 3.1 cm^2–19.1 cm^2. There was no significant difference between patients with and without recurrence, with regard to ROI size ($p = 0.11$ using the Mann-Whitney U-test).

Values of reference were obtained on the inferior one of the two tomograms selected. For this purpose, we determined the mean IMT uptake by the hemispherical half that was not affected by the tumor or, when the tumor had crossed the midline, by the anterior or posterior half of that brain slice. Pooling of the IMT uptake data, obtained using these different regions as reference, is possible because hemispherical, anterior or posterior halves of slices of IMT uptake do not differ significantly with regard to this variable (*12*).

Relative IMT uptake in the lesions was then determined by calculating ratios between the mean uptake in the two lesion ROIs and that in the reference ROI.

Because of the semiautomated nature of this approach, the intra- and interobserver reproducibility of this method of regional analysis has been shown to be very high, with correlation coefficients higher than 0.98 when relative uptake values determined by two different observers or by the same observer on two different days are compared (*12*).

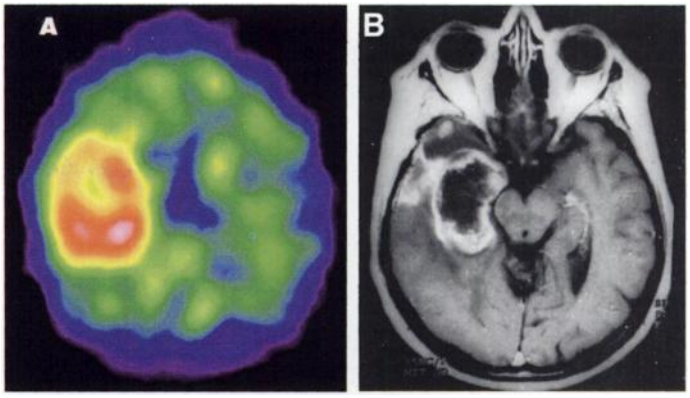

FIGURE 1. Minor IMT uptake in the contrast-enhancing rim of a postsurgical defect (A; transaxial) presented together with the corresponding postgadolinium T1-weighted MRI scan (B) in a patient without clinical deterioration during 13 mo of follow-up after surgery for a glioma IV (Patient 7; IMT uptake ratio = 1.49). The SPECT image is calibrated to its own maximum, with white and red indicating the highest values.

Relative IMT uptake values did not correlate significantly with ROI size (Spearman's correlation coefficient $r = -0.1$; $p > 0.5$).

All values are provided as mean ± s.d. P values of less than 0.05 were considered significant. The distribution of the IMT uptake values was compatible with normalcy, as assessed using Kolmogorov–Smirnoff one-sample tests. The significance of the difference in means of IMT uptake between the two groups was tested using the two-tailed Student's t-test (*20*).

We iteratively determined the threshold of discrimination between patients with and without recurrence that yielded the highest accuracy value (*21*). Sensitivity and specificity values were then calculated using standard formulas. Furthermore, using the software LABROC1, provided by Prof. C. Metz (Department of Radiology, University of Chicago, Chicago, IL), we fitted a binormal receiver operating characteristic (ROC) curve to our data (*22–24*).

RESULTS

The individual IMT uptake values are given in Table 1. Magnetic resonance imaging and IMT-SPECT scans of two representative patients are presented in Figures 1 and 2. Patients with recurrence had significantly higher ratios of IMT uptake in the tumor area to that in a background region than did patients without recurrence (2.27 ± 0.59 compared to 1.47 ± 0.29; $p < 0.002$).

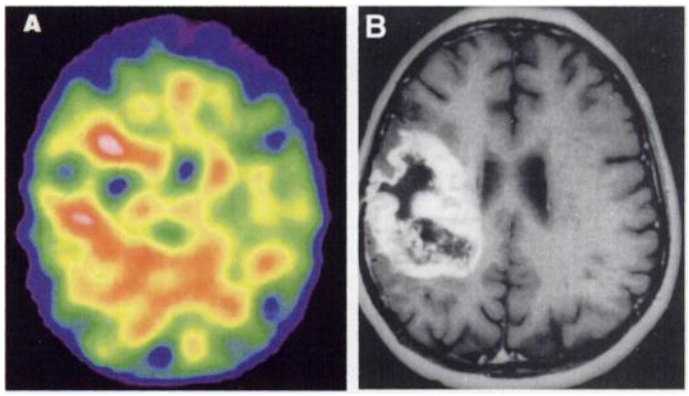

FIGURE 2. Marked IMT uptake in the contrast-enhancing rim of a postsurgical defect (A; transaxial) presented together with the corresponding T1-weighted postgadolinium MRI scan (B) in a patient with recurrence of a glioma IV (Patient 24; IMT uptake ratio = 2.24).

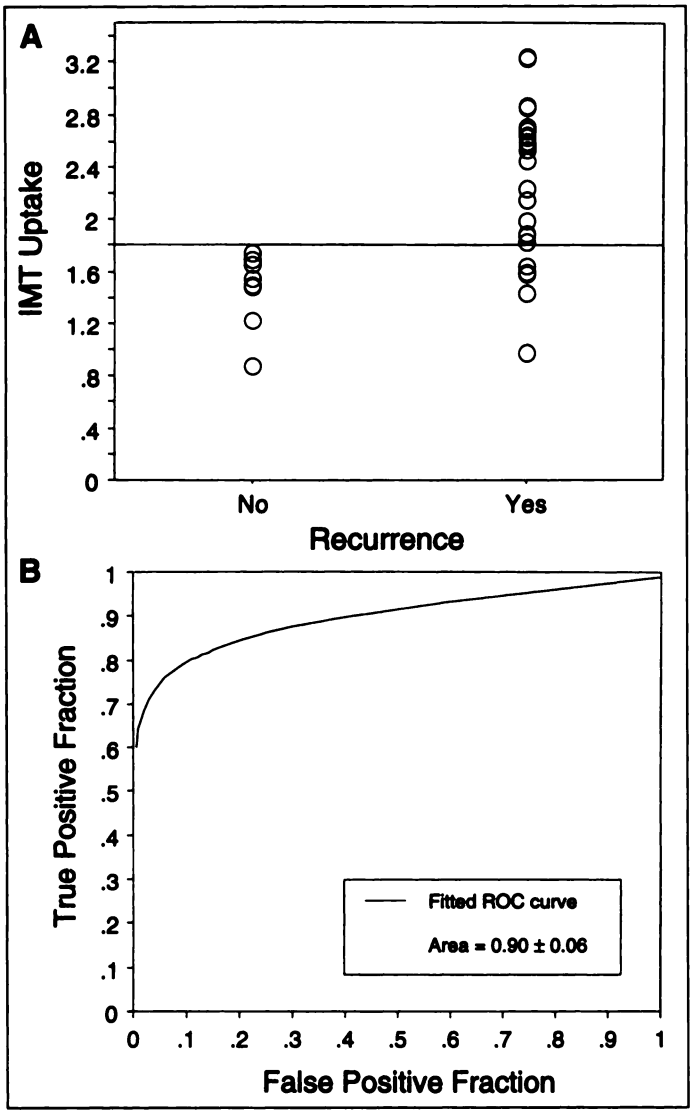

FIGURE 3. (A) Scatter diagram of relative IMT uptake in patients with and without glioma recurrence. The line denotes the discrimination threshold between these two groups. (B) Receiver operating characteristic curve for discrimination between patients with and without glioma recurrence.

The best cutoff level of the IMT uptake ratio in the differentiation between recurrence and benign posttherapeutic lesion was 1.8 (Fig. 3A). Using this threshold, the overall sensitivity and specificity for detecting glioma recurrence were 78% and 100%, respectively (Fig. 3A). The ROC curve is given in Figure 3B. The area under this curve, which is a commonly used figure of merit to evaluate the quality of a diagnostic test independently of an arbitrarily chosen threshold of discrimination, was 0.90 ± 0.06 (Fig. 3B).

DISCUSSION

The therapy of gliomas typically consists of a combination of surgery and radiation therapy (*1*). Therapeutic response is usually monitored with CT or MRI. However, CT and MRI have significant limitations when they are used to differentiate recurrent brain tumor from non-neoplastic abnormalities after treatment (*2–4*); in particular, with these techniques, it is difficult to differentiate between tumor recurrence and radiation necrosis because both these conditions may exhibit contrast enhancement and edema. Furthermore, brain regions already infiltrated by tumor cells may show no contrast enhancement on MRI or CT scans (*25*).

Using the recently introduced SPECT radiopharmaceutical IMT, we evaluated 31 studies from 27 patients on follow-up after surgery for gliomas. In our hands, the sensitivity and specificity of this method to differentiate recurrence from non-neoplastic posttherapeutic tissue abnormalities were 18 of 23 (78%) and 8 of 8 (100%), respectively.

Amino acid uptake can also be investigated with PET using amino acids labeled with positron-emitting isotopes (*26*). These PET amino acids and, in particular, [^{11}C]methionine have been widely used to study amino acid metabolism in brain tumors. The experience with these PET amino acids with regard to diagnosing brain tumor recurrence is limited (*27,28*). However, our data confirm results reported by Guth-Tougelides et al. (*29*) who used IMT-SPECT in a group of 16 patients after therapy for gliomas and correctly identified 14 of 17 recurrences and all three benign post-therapeutic lesions studied.

Various other radiopharmaceuticals are also being used in the follow-up of patients treated for brain tumors. Among these, FDG has been most extensively studied. The first results obtained using FDG-PET were indeed encouraging: Di Chiro et al. (*5*), who pioneered the use of FDG-PET in brain tumors, reported a nearly 100% accuracy of this method in a group of 95 patients studied after primary therapy of gliomas. Recent studies, however, have found lower sensitivity and specificity values for FDG-PET in this regard: Kahn et al. (*30*), for example, correctly identified only 11 of 16 tumor recurrences and 2 of 5 radiation necroses, corresponding to an 81% sensitivity and a 40% specificity. A possible interpretation of this discrepancy in results may be the introduction of more aggressive radiotherapy in these patients, leading to metabolically more active necrotic reactions in the brain or other differences in patient selection between these studies (*31*).

Other well-established radiopharmaceuticals that are suitable for differentiating between brain tumor recurrence and benign post-therapeutic lesions are ^{201}Tl and the isonitriles labeled with ^{99m}Tc, such as ^{99m}Tc-sestamibi (*32–35*). The sensitivity and specificity values for these two substances published in the literature are also in the range of those reported for FDG (*30*).

Presently, it is difficult to decide which of the different radiopharmaceuticals available is best-suited for diagnosing brain tumor recurrence. Although FDG and ^{201}Tl are well-established for this purpose, radioactively labeled amino acids may offer distinct advantages because they also accumulate, at least to some extent, in low-grade tumors (*12,36*) and in regions of the brain without contrast enhancement (*25,37*). Our results encourage further studies directly comparing the diagnostic utility of the different radiopharmaceuticals for this clinically important task.

One important issue in evaluating the diagnostic utility of radionuclide imaging for the diagnosis of brain tumor recurrence is the definition of the gold standard. First, some reservation should be applied to what is generally considered glioma recurrence because, in most cases, microscopic or even macroscopic remnants of the tumor remain within the brain even after extensive surgery; in these patients, which have not been cured by primary therapy, the question is when and not if the growth of these remnants becomes clinically apparent. Second, in an important subset of patients, a histological diagnosis was not available, as was also the case in 16 of our 27 patients. The reason for this is that biopsy or reoperation cannot be justified in all patients with brain tumor recurrence due to possible side effects of these invasive procedures and absence of therapeutic benefit. Furthermore, results from biopsy may be inaccurate in approximately 10% due to sampling errors (*38*). Therefore, in 16 of our patients and also in important subsets of

patients presented in some other articles (*6,30,31,35*), a distinction between recurrence and benign post-therapeutic lesions is based on the clinical course after radionuclide imaging. Mostly, a 6-mo follow-up is considered sufficient for this purpose because gliomas are proliferating within the restricted space of the skull. However, it cannot be excluded that particularly aggressive necrotic reactions after high-dose radiotherapy are mistaken for recurrences. Furthermore, an unremarkable 6-mo follow-up does not necessarily exclude a relapse after this period, particularly in low-grade neoplasms. Therefore, our data and those from other studies that rely on clinical course as gold standard should be interpreted with caution. However, our data do allow the conclusion that patients exhibiting high IMT uptake will deteriorate clinically within the near future. This information may help in patient counseling and also in planning biopsy and further therapeutic procedures.

CONCLUSION

IMT-SPECT is a promising new tool in the follow-up of patients with gliomas after primary therapy. The results presented encourage prospective studies comparing the value of IMT-SPECT with that of ^{201}Tl-SPECT and FDG-PET with regard to diagnosing recurrent glioma.

ACKNOWLEDGMENTS

We gratefully acknowledge the technical assistance of Anne Exler, Christine Papenberg and Silke Steinhoff; the provision of the ROC software by Prof. C. Metz and his colleagues from the Department of Radiology, University of Chicago (Chicago, IL); Prof. Altman's thorough revision of the manuscript; and the support by the late Prof. Peter E. Peters and Dr. Gerhard Schuierer from the Institut für Klinische Radiologie of the Westfälische Wilhelms-Universität (Münster, Germany).

REFERENCES

1. Schmidek HH. Surgical management of supratentorial gliomas. In: Schmidek HH, Sweet WH, eds. *Operative neurosurgical techniques*, 3rd ed. Philadelphia: W.B. Saunders; 1995:517–534.
2. Byrne TN. Imaging of gliomas. *Semin Oncol* 1994;21:162–171.
3. Leeds NE, Jackson EF. Current imaging techniques for the evaluation of brain neoplasms. *Curr Opin Oncol* 1994;6:254–261.
4. Dooms GC, Hecht S, Brant-Zawadzki M, et al. Brain radiation lesions: MR imaging. *Radiology* 1986;158:149–155.
5. Di Chiro G, Oldfield E, Wright DC, et al. Cerebral necrosis after radiotherapy and/or intraarterial chemotherapy for brain tumors. *Am J Roentgenol* 1988;150:189–197.
6. Glantz MJ, Hoffman JM, Coleman E, et al. Identification of early recurrence of primary central nervous system tumors by [^{18}F]fluorodeoxyglucose positron emission tomography. *Ann Neurol* 1991;29:347–355.
7. Biersack HJ, Coenen HH, Stöcklin G, et al. Imaging of brain tumors with L-3-[^{123}I]iodo-α-methyl tyrosine and SPECT. *J Nucl Med* 1989;30:110–112.
8. Langen K-J, Coenen HH, Roosen N, et al. SPECT studies of brain tumors with L-[^{123}I]iodo-α-methyl-tyrosine (^{123}IMT): first clinical results and comparison with PET and ^{124}IMT. *J Nucl Med* 1990;31:281–286.
9. Langen K-J, Roosen N, Coenen HH, et al. Brain and brain tumor uptake of L-[^{123}I]iodo-α-methyl-tyrosine: competition with natural L-amino acids. *J Nucl Med* 1991;32:1225–1228.
10. Kawai K, Fujibayashi Y, Saji H, et al. A strategy for the study of cerebral amino acid transport using an iodine-123-labeled amino acid radiopharmaceutical: 3-iodo-α-methyl-L-tyrosine. *J Nucl Med* 1991;32:819–824.
11. Kuwert T, Morgenroth C, Woesler B, et al. Influence of size of regions of interest on the measurement of uptake of iodine-123-α-methyl tyrosine by brain tumors. *Nucl Med Commun* 1996;17:609–615.
12. Kuwert T, Morgenroth C, Woesler B, et al. Uptake of iodine-123-α-methyl tyrosine by gliomas and non-neoplastic brain lesions. *Eur J Nucl Med* 1996;23:1345–1353.
13. Zülch KJ. Principles of the new World Health Organization (WHO) classification. *Neuroradiology* 1980;19:59–66.
14. Kuikka JT, Tenhunen-Eskelinen M, Jurvelin J, Kiliänen H. Physical performance of the Siemens Multi SPECT 3 gamma camera. *Nucl Med Commun* 1993;14:490–497.
15. Machulla HJ, Skansdal A, Stöcklin G. $^{123(125)}$Xe-exposed KIO3, a reagent for iodination with high specific activity. *Radioclin Acta* 1977;24:42–46.
16. Fischer S, Wolf H, Brandau W, Clausen M, Henze E, Schober O. Iodierung von α-methyltyrosin (AMT). Optimierung der methode für die routinepräparation [Abstract]. *Nuklearmedizin* 1993;32:A113.
17. Chang LT. A method for attenuation correction in radionuclide computed tomography. *IEEE Trans Nucl Sci* 1978;2:2780–2789.
18. Rottenberg DA, Moeller JR, Strother SC, Dhawan V, Sergi ML. Effects of percent thresholding on the extraction of [^{18}F]fluorodeoxyglucose positron emission tomographic region-of-interest data. *J Cereb Blood Flow* 1991;11:A83–A88.
19. Pruim J, Willemsen ATM, Molenaar WM, et al. Brain tumors: L-[1-C-11]tyrosine PET for visualization and quantification of protein synthesis rate. *Radiology* 1995;197:221–226.
20. Bortz J., ed. *Lehrbuch der statistik*, 2nd ed. Berlin: Springer-Verlag; 1985.
21. Delbeke D, Meyerowitz C, Lapidus RL, et al. Optimal cutoff levels of F-18 fluorodeoxyglucose uptake in the differentiation of low-grade from high-grade brain tumors with PET. *Radiology* 1995;195:47–52.
22. Dorfman DD, Alf E. Maximum likelihood estimation of parameters of signal detection theory and determination of confidence intervals: rating method data. *J Math Psychol* 1969;6:487–496.
23. Swets JA, Pickett RM, eds. *Evaluation of diagnostic systems: methods from signal detection theory*. New York: Academic Press, 1982.
24. Metz CE. Some practical issues of experimental design and data analysis in radiological ROC studies. *Invest Radiol* 1989;24:234–245.
25. Mosskin S, Ericson K, Hindmarsh T, et al. Positron emission tomography compared with magnetic resonance imaging and computed tomography in supratentorial gliomas using multiple stereotactic biopsies as reference. *Acta Radiol* 1989;30:225–232.
26. Herholz K. Tracers for clinical evaluation of gliomas: a neurologist's view. In: Mazoyer BM, Heiss WD, Comar D, eds. *PET studies on amino acid metabolism and protein synthesis*. Dordrecht, The Netherlands: Kluwer Academic Publishers; 1993; 203–214.
27. Lilja A, Lundquist H, Olsson Y, et al. Positron emission tomography and computed tomography in differential diagnosis between recurrent or residual glioma and treatment induced brain lesions. *Acta Radiol* 1989;30:121–128.
28. Ogawa T, Kanno I, Shishido F, et al. Clinical value of PET with ^{18}F-fluorodeoxyglucose and L-methyl-^{11}C-methionine for diagnosis of recurrent brain tumor and radiation injury. *Acta Radiol* 1991;32:197–202.
29. Guth-Tougelides B, Müller St, Mehdorn MM, Knust EJ, Dutschka K, Reiners C. Anreicherung von DL-3-^{123}I-jod-α-methyltyrosin in hirntumorrezidiven. *Nuklearmedizin* 1995;34:71–75.
30. Kahn D, Follett KA, Bushnell DL, et al. Diagnosis of recurrent brain tumor: value of ^{201}Tl-SPECT vs. ^{18}F-fluorodeoxyglucose PET. *Am J Roentgenol* 1994;163:1459–1465.
31. Janus TJ, Kim E, Tilbury R, Bruner JM, Yung WKA. Use of [^{18}F]fluorodeoxyglucose positron emission tomography in patients with primary malignant brain tumors. *Ann Neurol* 1993;33:540–548.
32. Kaplan WD, Takronan T, Morris H, et al. Thallium-201 brain tumor imaging: a comparative study with pathologic correlation. *J Nucl Med* 1987;28:47–52.
33. Mountz JM, Stafford-Schuck K, McKeever PE, et al. Thallium-201 tumor/cardiac ratio estimation of residual astrocytoma. *J Neurosurg* 1988;68:705–709.
34. Carvalho PA, Schwartz RB, Eben A, et al. Detection of recurrent gliomas with quantitative thallium-201/technetium-99m HMPAO single-photon emission computerized tomography. *J Neurosurg* 1992;77:565–570.
35. Maffioli L, Gasparini M, Chiti A, et al. Clinical role of technetium-99m sestamibi single-photon emission tomography in evaluating pretreated patients with brain tumors. *Eur J Nucl Med* 1996;23:308–311.
36. Ericson K, Lilja A, Bergström M, et al. Positron emission tomography with ([^{11}C]methyl)-L-methionine, [^{11}C]D-glucose, and [^{68}Ga]EDTA in supratentorial tumors. *J Comput Assist Tomogr* 1985;9:683–689.
37. Ogawa T, Miura S, Murakami M, et al. Quantitative evaluation of neutral amino acid transport in cerebral gliomas using positron emission tomography and fluorine-18 fluorophenylalanine. *Eur J Nucl Med* 1996;23:889–895.
38. Paulus W, Peiffer J. Intratumoral histologic heterogeneity of gliomas. A quantitative study. *Cancer* 1989;64:442–447.